

Misfolded PrP impairs the UPS by interaction with the 20S proteasome and inhibition of substrate entry

Pelagia Deriziotis^{1,6,7}, Ralph André^{1,6},
David M Smith^{2,3,6}, Rob Gooled¹,
Kerri J Kinghorn¹, Mark Kristiansen⁴,
James A Nathan², Rina Rosenzweig⁵,
Dasha Krutauz⁵, Michael H Glickman⁵,
John Collinge^{1,4}, Alfred L Goldberg²
and Sarah J Tabrizi^{1,*}

¹Department of Neurodegenerative Disease, University College London Institute of Neurology, Queen Square, London, UK, ²Department of Cell Biology, Harvard Medical School, Boston, MA, USA, ³Department of Biochemistry, West Virginia University School of Medicine, Medical Center Drive, Morgantown, WV, USA, ⁴MRC Prion Unit, University College London Institute of Neurology, Queen Square, London, UK and ⁵Department of Biology, Technion—Israel Institute of Technology, Haifa, Israel

Prion diseases are associated with the conversion of cellular prion protein (PrP^C) to toxic β -sheet isoforms (PrP^{Sc}), which are reported to inhibit the ubiquitin-proteasome system (UPS). Accordingly, UPS substrates accumulate in prion-infected mouse brains, suggesting impairment of the 26S proteasome. A direct interaction between its 20S core particle and PrP isoforms was demonstrated by immunoprecipitation. β -PrP aggregates associated with the 20S particle, but did not impede binding of the PA26 complex, suggesting that the aggregates do not bind to its ends. Aggregated β -PrP reduced the 20S proteasome's basal peptidase activity, and the enhanced activity induced by C-terminal peptides from the 19S ATPases or by the 19S regulator itself, including when stimulated by polyubiquitin conjugates. However, the 20S proteasome was not inhibited when the gate in the α -ring was open due to a truncation mutation or by association with PA26/PA28. These PrP aggregates inhibit by stabilising the closed conformation of the substrate entry channel. A similar inhibition of substrate entry into the proteasome may occur in other neurodegenerative diseases where misfolded β -sheet-rich proteins accumulate.

The EMBO Journal (2011) 30, 3065–3077. doi:10.1038/emboj.2011.224; Published online 8 July 2011

Subject Categories: proteins; molecular biology of disease

Keywords: neuroscience; prion; proteasome; PrP; UPS

*Corresponding author. Department of Neurodegenerative Disease, University College London Institute of Neurology, Queen Square, London WC1N 3BG, UK. Tel.: +44 845 155 5000/ext. 724434; Fax: +44 207 676 2180; E-mail: sarah.tabrizi@prion.ucl.ac.uk

⁶These authors contributed equally to this work

⁷Present address: Wellcome Trust Centre for Human Genetics, Roosevelt Drive, University of Oxford, Oxford, UK

Received: 1 November 2010; accepted: 16 June 2011; published online: 8 July 2011

Introduction

Prion diseases are fatal neurodegenerative disorders whose pathogenesis is associated with a conformational rearrangement of the normal cellular prion protein (PrP^C) to abnormal infectious isoforms (PrP^{Sc}) (Prusiner, 1982). Neuropathological findings include spongiform change, marked neuronal loss and astrogliosis, and the accumulation of PrP^{Sc} in the brain. Although they share the same amino-acid sequence, PrP^C is mainly α -helical, whereas PrP^{Sc} is β -sheet rich. Also, PrP^{Sc} is less soluble in detergents and more resistant to proteases (Prusiner, 1998). To date, the cause of prion-mediated neurodegeneration remains unclear. Although PrP^C is essential for prion disease development, PrP^C knockout mice show no gross pathology (Bueler *et al*, 1993; Mallucci *et al*, 2002). Therefore, loss of PrP^C function is not the cause of prion-mediated cell death and pathology must result from a toxic gain-of-function associated with conversion of PrP^C to β -sheet-rich PrP^{Sc}. Indeed, many pathways have been proposed to explain precise mechanisms of neuronal cell death in prion disease (Caughey and Baron, 2006; Collinge and Clarke, 2007; Tatzelt and Schatzl, 2007).

Evidence suggests that functional impairment in the ubiquitin-proteasome system (UPS) may be important in prion diseases (Deriziotis and Tabrizi, 2008). This pathway catalyses the rapid elimination of misfolded cell proteins and many proteins critical in regulating gene expression and metabolism (Goldberg, 2003). In the UPS, protein substrates are covalently linked to a polyubiquitin chain, which leads to rapid binding and degradation by the 26S proteasome (Glickman and Ciechanover, 2002). This ATP-dependent proteolytic complex consists of the 20S core particle and one or two 19S regulatory particles. The 20S proteasome is a barrel-shaped complex within which substrates are degraded. It is composed of four stacked rings, containing seven α -subunits in the two outer rings and seven β -subunits in the two inner rings. Three of these β -subunits have peptidase activity (Glickman and Ciechanover, 2002): the β_1 -subunits have caspase-like activity, β_2 -subunits have trypsin-like activity and β_5 -subunits have chymotrypsin-like activity. The N-termini of the α -subunits function as a gate into the proteolytic chamber and block substrate entry (Groll *et al*, 2000; Smith *et al*, 2007; Gillette *et al*, 2008; Rabl *et al*, 2008). The six ATPase subunits that comprise the base of the 19S (Rpt1-6) regulate gate opening in the 20S proteasome, which leads to increased entry and hydrolysis of peptides and unfolded proteins (Kohler *et al*, 2001; Smith *et al*, 2005).

Impairment of the UPS has also been suggested to contribute to the pathogenesis of neurodegenerative conditions such as Huntington's disease (HD), Parkinson's disease (PD) and Alzheimer's disease (AD) (Rubinsztein, 2006). In these diseases, misfolded proteins accumulate as aggregated intraneuronal inclusions or as neurofibrillary tangles, which contain ubiquitin and proteasomes. Conditional depletion of 26S

proteasomes in neurons of the substantia nigra or forebrain in mice results in neurodegeneration with inclusions resembling Lewy bodies in PD (Bedford *et al*, 2008). In prion disease, prion-infected mouse brains have increased levels of ubiquitin conjugates, which correlate with decreased proteasome function (Kang *et al*, 2004); and the *Hectd2* gene which encodes a ubiquitin ligase, was identified as a gene influencing incubation time for prion disease in mice (Lloyd *et al*, 2009).

Increasing evidence suggests that soluble micro-aggregates of misfolded proteins, rather than larger protein inclusions, are toxic to neurons in these diseases (Rubinsztein, 2006). It is possible that the build-up of such aggregates eventually overwhelms the UPS, causing a functional impairment. We reported that aggregated β -sheet-rich PrP oligomers inhibit the proteolytic activities of the 26S proteasome, an effect specific to PrP in an aggregated, non-native β -sheet conformation (Kristiansen *et al*, 2007). By contrast, the recombinant protein in a PrP^C-like conformation and other fibrillar amyloidogenic proteins was not inhibitory. Using a transgenic mouse model expressing a short-lived reporter protein (Lindsten *et al*, 2003), we presented further evidence for impairment of the UPS in prion-infected brains (Kristiansen *et al*, 2007). Therefore, impairment of the UPS may have an important role in prion and other neurodegenerative diseases characterised by accumulation of misfolded proteins, but the biochemical mechanisms underlying this dysfunction remain unclear.

Inactivation of any one of the three active sites of the 20S proteasome slows, but does not block, protein degradation; in fact, in order to impair protein degradation significantly, the chymotrypsin-like sites as well as either the caspase-like or the trypsin-like sites need to be inhibited (Kisselev *et al*, 2006). We found previously that aggregated β -sheet-rich PrP isoforms inhibit peptide hydrolysis by all these sites, although the trypsin-like activity was inhibited to a lesser extent (Kristiansen *et al*, 2007). There are two possible explanations for these effects. First, the aggregated PrP species may enter the 20S particle and directly inhibit its three active sites. This mechanism seems unlikely as the pore of the 20S barrel does not exceed 2 nm in diameter (Groll *et al*, 2000); consequently, aggregated proteins should not be able to enter this particle. Alternatively, PrP isoforms may inhibit the entry of protein and peptide substrates into the 20S proteasome perhaps by blocking gate opening by the regulatory ATPases. Such an effect should reduce its ability to digest proteins as well as small peptide substrates, but to varying extents. In fact, Kisselev *et al* (2002) showed that agents or mutations that promote gate opening enhance most dramatically the hydrolysis of hydrophobic and acidic peptides whose breakdown is limited by entry into the particle, but have lesser effects on hydrolysis of basic peptides which is limited by the slow turnover rate of the trypsin-like site (Kisselev *et al*, 2002). Therefore, an inhibitory effect of the aggregated PrP on gate opening should result in a more marked reduction in the chymotrypsin-like and caspase-like activities, as was observed (Kristiansen *et al*, 2007).

The aim of the present study was to determine how aggregated β -sheet-rich PrP species interact with the proteasome and inhibit its function. Here, we present evidence that they inhibit by decreasing gate opening in the 20S particle, leading to a reduced capacity of the proteasomes to degrade

peptides and proteins. We also demonstrate that PrP isoforms directly interact with the 26S proteasome both *in vitro* and *in vivo*, and cause an accumulation of key UPS substrates in prion-infected mouse brains. This ability of aggregated β -sheet-rich PrP isoforms to block substrate entry into the 20S proteasome may be a model for understanding pathogenic mechanisms in other neurodegenerative diseases, where there is also an accumulation of misfolded β -sheet-rich proteins and impairment of protein degradation.

Results

Key UPS substrates accumulate in prion-infected mouse brain

Previously, we presented evidence that the UPS is impaired in prion-infected brains of transgenic mice expressing a short-lived reporter protein (Kristiansen *et al*, 2007). In order to confirm that the UPS was impaired *in vivo*, we assayed the levels of three important substrates. During inflammation, I κ B is a rapidly degraded proteasomal substrate that accumulates upon treatment of cells with proteasome inhibitors (Palombella *et al*, 1994). Assays of I κ B α levels by western blot in RML prion-infected mouse brains revealed a significant accumulation above those in matched controls (Figure 1A). Levels of two additional endogenous proteasomal substrates, the cyclin-dependent kinase inhibitor, p27 (Figure 1B), and the p53 tumour suppressor protein (Figure 1C), were also significantly greater in RML prion-infected mouse brains than in matched controls. Since there was no significant difference in transcript expression between prion-infected and control brains (Supplementary Figure S1), the increased levels of I κ B α , p27 and p53 are most likely due to reduced proteasomal function.

PrP^{Sc} and 26S proteasome components associate with each other *in vivo*

To investigate whether PrP^{Sc} binds to the 26S proteasome during infection *in vivo*, we tested if anti-PrP antibody (Ab)-coated beads could co-immunoprecipitate 26S components from prion-infected brain. We observed that PrP co-immunoprecipitated both the 20S particle and the 19S subunit, Rpt1, in RML prion-infected mouse brain (Figure 2A). It could also be seen to co-immunoprecipitate another 19S subunit, Rpn7 (Supplementary Figure S2). In similar experiments, anti-20S Ab-coated beads co-immunoprecipitated PrP from an RML prion-infected mouse brain fraction (Figure 2B). The immunoprecipitate was then analysed by immunoblotting with an anti-PrP antibody either directly (Figure 2B, middle) or after proteinase K (PK) digestion (Figure 2B, bottom), which revealed the triplet of protease-resistant bands characteristic of prion disease-associated PrP^{Sc}. Control experiments using BSA-coated beads did not precipitate any proteins (Figure 2A and B). These results indicate a specific association between PrP^{Sc} and 26S proteasome components in prion-infected brains.

Aggregated β -PrP binds directly to human 20S and 26S proteasomes

Full-length recombinant mouse PrP (aa23-231) was folded into either an α -helical structure representative of native PrP^C (α -PrP), or a predominantly β -sheet species, termed β -PrP, that has similar physico-chemical properties to PrP^{Sc}

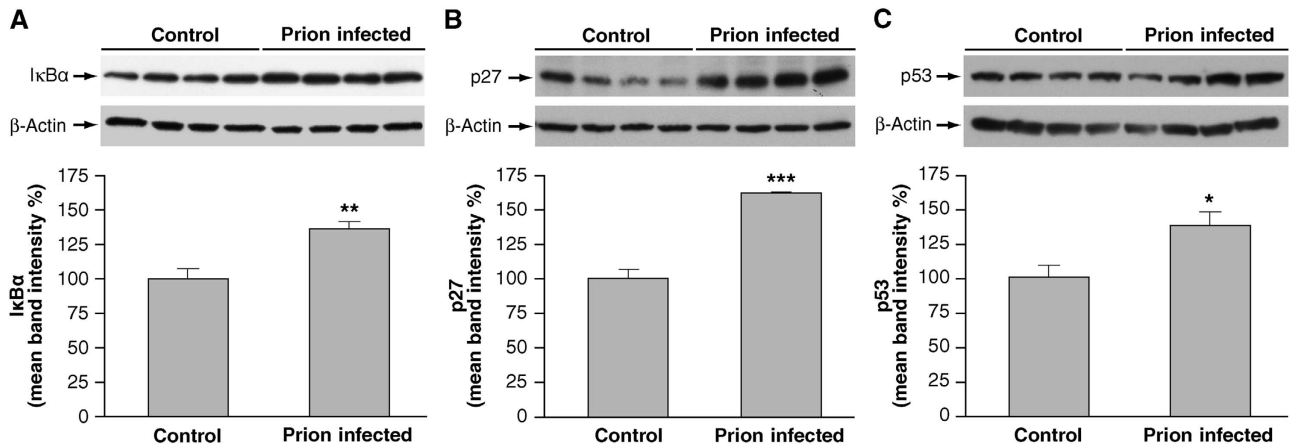


Figure 1 Accumulation of substrates of the UPS occurs in prion-infected mouse brains. (A) IκBα, (B) p27 and (C) p53 levels are significantly increased, assessed by immunoblot relative to β-actin expression, in four end-stage prion-infected mouse brain homogenates as compared with four uninfected controls (***P*<0.001, ***P*<0.01, and **P*<0.05, respectively).

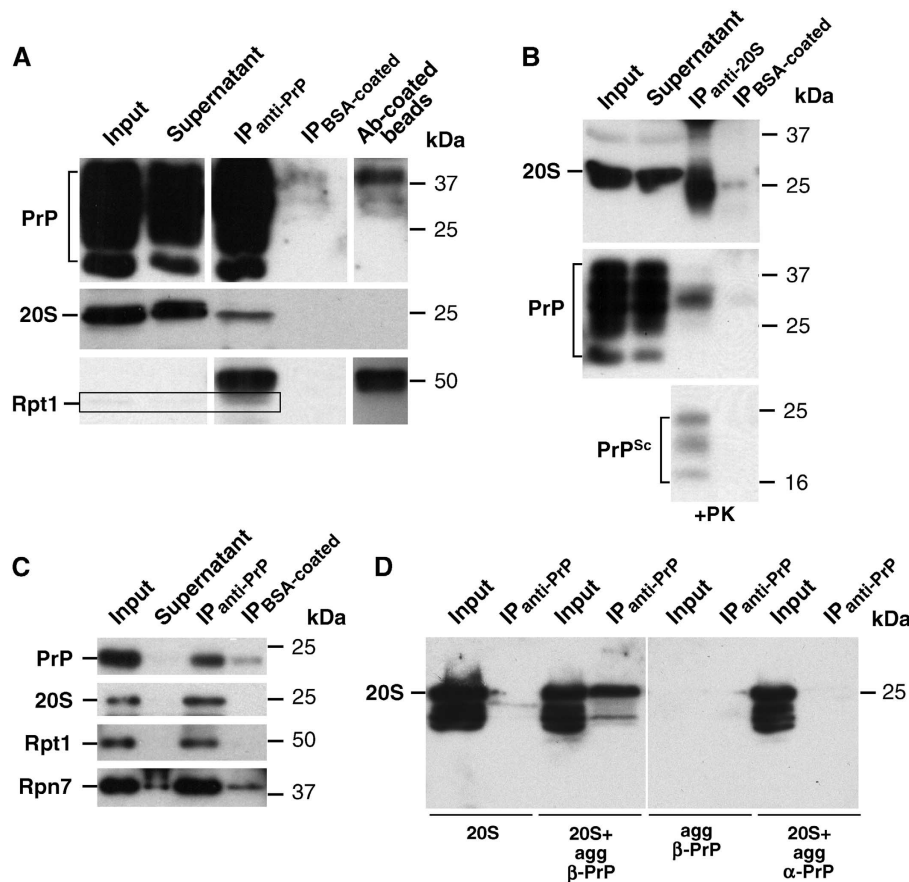


Figure 2 PrP^{Sc} and 26S components co-immunoprecipitate. (A) 20S proteasomes and 19S components co-precipitate with PrP from prion-infected mouse brain using anti-PrP antibody-coated beads. Immunoprecipitated (IP_{anti-PrP}), control (using beads coated with BSA alone; IP_{BSA-coated}) and unbound (supernatant) fractions, together with starting material (input) and antibody-coated beads alone (Ab-coated beads), were immunoblotted with anti-PrP, anti-20S and anti-Rpt1 antibodies. Boxed areas highlight specific bands as distinct from immunoglobulin chains eluted from the antibody-coated beads. An increased proportion of the IP fraction was loaded for detection of Rpt1. Separate panels showing images as detected by the same antibody are from the same immunoblot. (B) PrP^{Sc} co-precipitates with the 20S particle from prion-infected mouse brain using anti-20S antibody-coated beads. IP_{anti-20S}, control (IP_{BSA-coated}) and unbound (supernatant) fractions, and input starting material, were immunoblotted with anti-PrP and anti-Rpt1 antibodies. The characteristic triplet of protease-resistant bands revealed by proteinase K (+PK) digestion of the IP_{anti-20S} fraction demonstrates the presence of PrP^{Sc}. Aggregated β-PrP binds directly to 20S and 19S components. (C) 20S and 19S components co-precipitate with PrP when human 26S proteasomes are incubated with aggregated β-PrP for 1 h at 37°C and immunoprecipitated using anti-PrP antibody-coated beads. IP_{anti-PrP}, control (IP_{BSA-coated}) and unbound (supernatant) fractions, together with input starting material, were immunoblotted with anti-PrP, anti-20S, anti-Rpt1 and anti-Rpn7 antibodies. (D) 20S proteasome co-precipitates with PrP when human 20S proteasomes are incubated with aggregated β-PrP for 1 h at 37°C, but not when incubated with aggregated α-helical PrP. The IP_{anti-PrP} fraction and input starting material were immunoblotted with an anti-20S antibody. No 20S subunits were detected in the aggregated β-PrP-only control. The anti-20S antibody used to visualise the 20S recognises the following subunits: α₅/α₇, β₁, β₅ and β₇.

(Jackson *et al*, 1999b), as described previously (Kristiansen *et al*, 2007). To determine whether PrP interacts directly with the 26S proteasome, we incubated purified human 26S particles with aggregated β -PrP and then added anti-PrP Ab-coated beads. 20S proteasome and 19S components (Rpt1 and Rpn7) were precipitated by the anti-PrP antibody (Figure 2C). Control experiments using BSA-coated beads did not precipitate significant amounts of any 26S proteasome components (Figure 2C). In similar experiments, human 20S proteasomes were incubated with either aggregated β -PrP or heat-aggregated α -PrP before incubation with the anti-PrP Ab-coated beads. 20S subunits were precipitated by the anti-PrP antibody in the presence of aggregated β -PrP, but not with aggregated α -PrP (Figure 2D). These results demonstrate that aggregated β -PrP has a high affinity for the 20S particle, suggesting a strong interaction between β -sheet-rich PrP species and 20S proteasomes.

β -Sheet-rich PrP isoforms inhibit degradation of casein

To assess the functional relevance of prion-induced inhibition of the UPS, we measured the effects of different PrP isoforms on the degradation of a model protein substrate, FITC-casein, by purified 20S proteasomes (Kisselev *et al*, 1999). Pre-incubating yeast 20S proteasomes with aggregated β -PrP markedly reduced the degradation of casein and this inhibitory effect was dependent on the amount of β -PrP added (Figure 3A). When an equal amount of aggregated α -PrP was added, there was little or no inhibition of FITC-casein degradation (Figure 3B), showing that aggregation *per se* is not sufficient.

Low concentrations of aggregated PrP inhibit peptide hydrolysis by the 20S proteasome

Our previous data suggested that the inhibitory species are small aggregates of oligomeric β -sheet-rich PrP (Kristiansen *et al*, 2007). To further define this inhibition, we monitored the chymotrypsin-like activity of wild-type

yeast 20S proteasomes after incubation with increasing amounts of aggregated β -PrP. Half-maximal inhibition of the 20S particles was observed at between 90 and 180 nM aggregated β -PrP, where concentrations are calculated based upon the total amount of free monomeric protein added (Figure 4A). However, because most of the β -PrP is aggregated, the actual number of free molecules in solution must be much lower. Since the concentration of 20S proteasomes in the reactions was 9 nM, the affinity of aggregated β -PrP for the proteasome must be quite high.

β -Sheet-rich PrP isoforms inhibit wild-type 20S proteasomes, but not an open-gated mutant

As protein aggregates cannot enter the narrow 13 Å channel into the 20S proteasome, and therefore should not interact directly with its proteolytic sites, we tested whether aggregated β -sheet-rich PrP isoforms inhibit opening of the gated substrate entry channel in the 20S proteasome α -ring. To examine this possibility, we tested the ability of β -sheet-rich PrP isoforms to inhibit a variant of the 20S proteasome that contains a constitutively open gate ($\alpha 3\Delta N$ -20S) by means of a nine residue truncation of its $\alpha 3$ N-terminus (Groll *et al*, 2000). This deletion prevents formation of the closed-gate conformation. Proteasome inhibitors that block the proteolytic sites can readily inhibit the 'open-gated' mutant 20S proteasome, but if agents affect gate opening, they should not be able to influence the peptidase activity of this mutant.

When aggregated β -PrP or PrP^{Sc} isolated from prion-infected mouse hypothalamic neuronal cells (ScGT-1; Kristiansen *et al*, 2007) were incubated with wild-type 20S proteasomes, both caused a significant reduction in all three peptidase activities (Figure 4B). By contrast, in the $\alpha 3\Delta N$ mutant 20S particles, these PrP species had no effect on peptide hydrolysis by the three different active sites (Figure 4C). To confirm that the mutant $\alpha 3\Delta N$ 20S proteasomes had an open gate, we compared its basal activity with that of the wild-type 20S particle. As expected, these

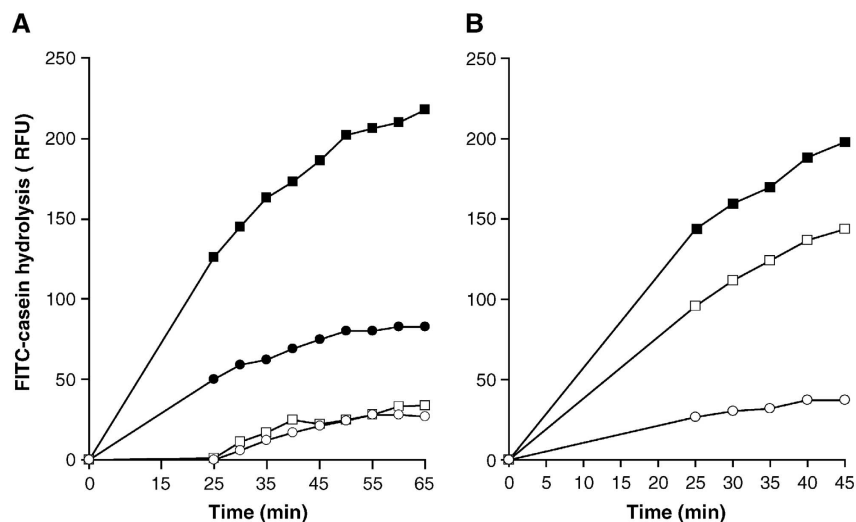


Figure 3 β -Sheet-rich PrP species inhibit casein degradation by purified 20S proteasomes. (A) Increasing concentrations of aggregated β -PrP (■ = control; ● = 250 μ g/ml; □ = 500 μ g/ml; ○ = 1 mg/ml) decrease the degradation rate of FITC-labelled casein by wild-type yeast 20S proteasomes. (B) Aggregated α -helical PrP causes much less inhibition than aggregated β -PrP (■ = wild-type 20S alone; □ = 1 mg/ml α -PrP; ○ = 1 mg/ml β -PrP). The molar ratio in these reactions of 1 mg/ml PrP to yeast 20S proteasomes is 69:1 based upon the total amount of free monomeric PrP added. Each graph is representative of at least three independent experiments.

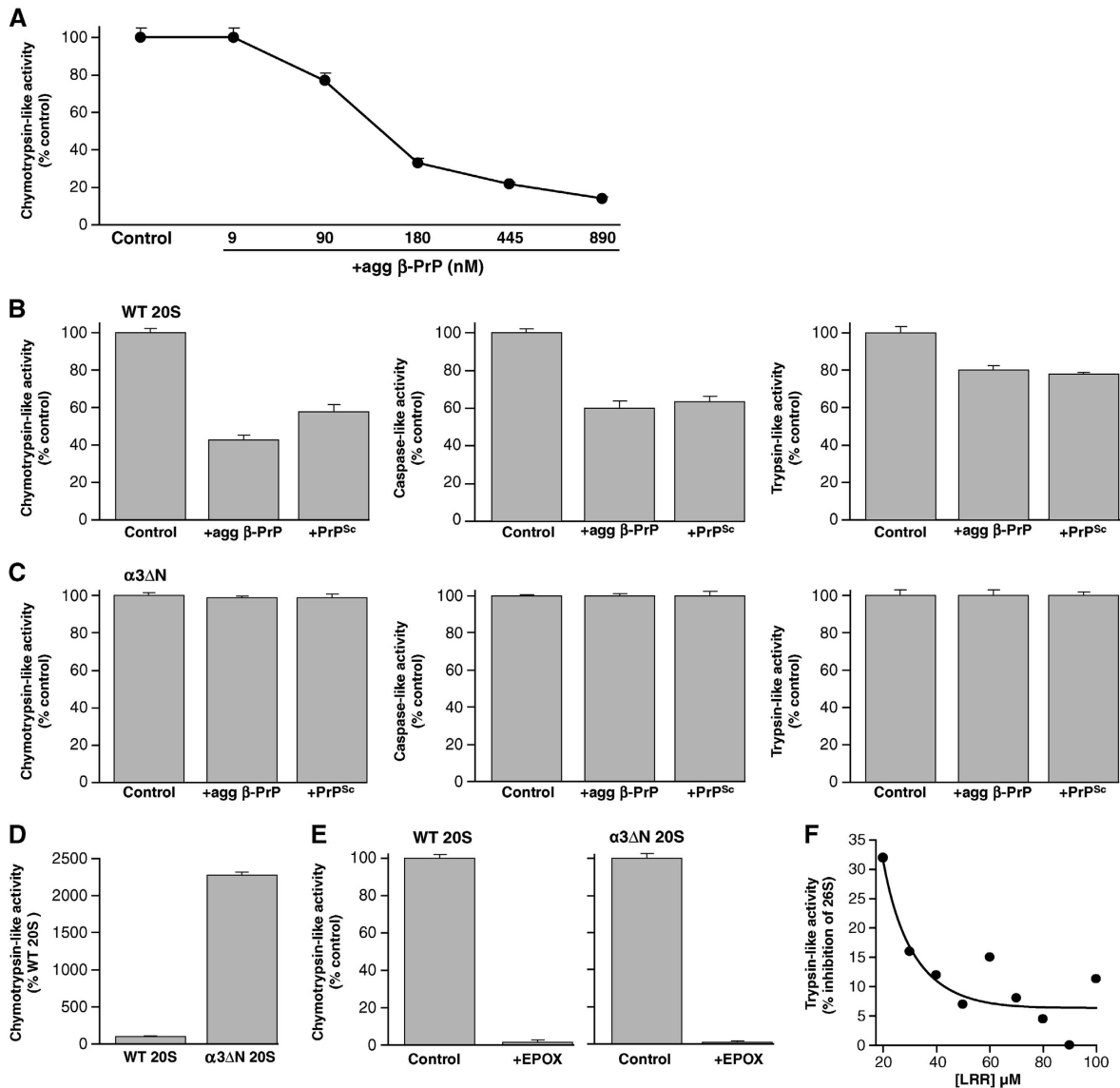


Figure 4 β -Sheet-rich PrP species inhibit wild-type yeast 20S proteasomes, but not an open-gated 20S mutant. (A) Half-maximal inhibition of wild-type yeast 20S proteasomes (9 nM) is observed between 90 and 180 nM aggregated β -PrP (molar concentrations are based upon the free monomeric protein added). (B) Aggregated β -PrP (20 μ g/ml) or PrP^{Sc} semi-purified from RML prion-infected ScGT-1 cells (20 μ g/ml) inhibits all three peptidase activities of the wild-type yeast 20S proteasomes ($P < 0.001$ versus respective controls). (C) Aggregated β -PrP and semi-purified PrP^{Sc} have no inhibitory effect on the activities of the open-gated $\alpha 3\Delta N$ yeast 20S mutant. (D) As expected for an open-gated mutant, $\alpha 3\Delta N$ 20S particles show much higher basal chymotrypsin-like activity compared with wild-type 20S. (E) Chymotrypsin-like activity is abolished in both wild-type 20S and $\alpha 3\Delta N$ 20S mutant proteasomes after pre-treatment with 50 μ M epoxomicin (EPOX), a specific proteasome inhibitor. (F) The inhibitory effect of aggregated β -PrP on the trypsin-like activity of the 26S proteasome was seen at low substrate concentrations and not at high concentrations. Human 26S proteasomes were incubated with or without 20 μ g/ml aggregated β -PrP, before the addition of Boc-LRR-amc substrate (ranging from 20 to 100 μ M) to monitor trypsin-like activity.

open-gated mutants showed much higher basal activity (Figure 4D). In addition, the peptidase activities we monitored were specific to the proteasome, since addition of the specific proteasome inhibitor, epoxomicin, completely abolished the chymotrypsin-like activity of these preparations (Figure 4E). These data imply that aggregated β -sheet-rich PrP species inhibit gate opening in the 20S proteasome, which can account for the previously described inhibition of 26S proteasomal function (Kristiansen *et al*, 2007).

Aggregated β -PrP binds open-gated mutant 26S proteasomes

As was found using the 20S particles (Figure 4), aggregated β -PrP significantly reduced the chymotrypsin-like activity of

wild-type 26S proteasomes, but did not inhibit the activity of open-gated $\alpha 3\Delta N$ 26S particles (Figure 5A). Possibly this failure to inhibit the open-gated $\alpha 3\Delta N$ proteasomes could be due to an inability to bind to the mutant particles. To assess whether aggregated β -PrP associates directly with open-gated $\alpha 3\Delta N$ 26S proteasomes, we used anti-PrP Ab-coated beads to test if the $\alpha 3\Delta N$ mutant 26S could be co-immunoprecipitated from these reactions. When wild-type and $\alpha 3\Delta N$ 26S proteasomes were incubated with aggregated β -PrP, and then incubated with anti-PrP Ab-coated beads, the 20S core components were precipitated (Figure 5B). Control experiments using BSA-coated beads did not precipitate the 20S components (Figure 5B). Thus, although aggregated β -PrP binds to the constitutively open-gated $\alpha 3\Delta N$ mutant

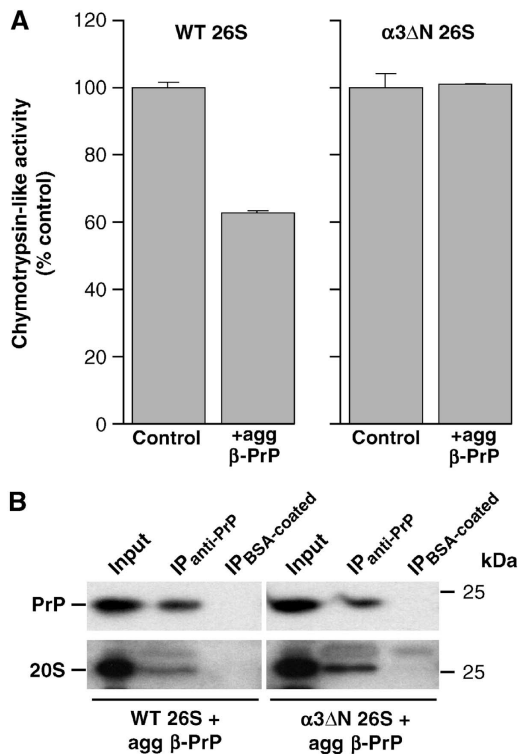


Figure 5 Aggregated β -PrP binds directly to both wild-type yeast 26S proteasomes and an open-gated 26S mutant. **(A)** Aggregated β -PrP (50 μ g/ml) inhibits chymotrypsin-like activity of wild-type yeast 26S proteasome ($P < 0.001$ versus relative control), but not the open-gated α 3 Δ N 26S mutant. **(B)** 20S components co-precipitate with PrP when either wild-type or α 3 Δ N yeast 26S proteasomes are incubated with aggregated β -PrP for 1 h at 37°C and immunoprecipitated using anti-PrP antibody-coated beads. Immunoprecipitated (IP_{anti-PrP}) and control (IP_{BSA-coated}) fractions, together with the starting material (input), were immunoblotted with anti-PrP and anti-20S antibodies.

proteasomes, it fails to inhibit substrate entry and degradation. Therefore, β -PrP must inhibit proteasome function by acting on the gating mechanism.

Effects on trypsin-like activity also suggest reduced substrate entry

These findings, and ones below, indicate that misfolded PrP inhibits the 20S proteasome gating mechanism, and therefore should reduce the hydrolysis of all substrates. However, in most experiments, peptide substrates of the chymotrypsin and caspase sites are inhibited more by aggregated β -PrP than those of the trypsin sites (see Figures 4B and 6). In fact, the rate of substrate cleavage by the chymotrypsin-like and caspase-like sites is more sensitive to gate opening than by the trypsin-like site (Kisselev *et al*, 2002). This is because gate opening will only enhance substrate hydrolysis if its rate of diffusion into the 20S particle is slower than its rate of cleavage by the active sites, and the trypsin-like site has a much lower turnover rate than the other active sites. Consequently, the entry of its substrates is typically not rate limiting for degradation, but can be made rate limiting by lowering the concentration of its substrates, for example, Boc-LRR-amc (Kisselev *et al*, 2002). If the β -sheet-rich PrP isoforms inhibit the cleavage of this substrate of the trypsin-like sites by blocking gate opening, the aggregated β -PrP should

reduce its hydrolysis at low, but not at higher concentrations. Accordingly, aggregated β -PrP was more inhibitory at lower Boc-LRR-amc concentrations (Figure 4F), where entry into the particle becomes rate limiting. These findings further support our conclusion that the PrP species are inhibiting proteasome function by reducing substrate entry into the 20S particle.

Aggregated β -sheet-rich PrP isoforms inhibit Rpt5-stimulated 20S proteasomes

Gate opening in the 26S proteasome is regulated such that when the 19S ATPase subunits, Rpt2 and Rpt5, bind ATP, their C-termini dock into intersubunit pockets in the 20S particle α -ring and induce gate opening. This effect requires a conserved HbYX motif in the C-termini (Smith *et al*, 2007; Gillette *et al*, 2008; Rabl *et al*, 2008), which interacts with residues in these pockets. To investigate whether aggregated β -sheet-rich PrP isoforms can inhibit this gate opening process, we used a synthetic 8-residue peptide (KANLQYYA) corresponding to the C-terminus of the mammalian Rpt5 subunit (termed Rpt5), which has previously been shown to induce gate opening (Smith *et al*, 2007). As expected, this C-terminal peptide strongly induced gate opening in human 20S proteasomes, since it stimulated substrate cleavage by all three proteolytic sites (Figure 6; Supplementary Figure S3).

We then examined whether pre-incubating these particles with aggregated β -sheet-rich PrP species affects their response to the gate opening peptide. Both aggregated β -PrP (Figure 6A) and semi-purified PrP^{Sc} (Supplementary Figure S3A) blocked much of the Rpt5-induced increase in peptide entry, even though the Rpt5 peptide was present in a 25-fold molar excess over the total amount of β -sheet-rich PrP isoforms added. Furthermore, when the Rpt5 activator was added *before* the aggregated β -PrP or PrP^{Sc}, the aggregated β -sheet-rich PrP species caused a similar reduction in activation of 20S proteasomes (Figure 6B; Supplementary Figure S3B). In agreement with our previous findings (Kristiansen *et al*, 2007), substrate entry was inhibited only by the specific pathogenic conformation of β -PrP and PrP^{Sc}, as neither heat-denatured β -PrP, denatured PrP^{Sc} nor heat-aggregated α -PrP were inhibitory (Supplementary Figure S3C).

However, it should be noted, as shown in Figure 6A, the inhibition of substrate entry by the aggregated β -PrP is primarily due to a large decrease in basal gate opening. When the β -PrP was present, the addition of Rpt5 peptide still caused a large stimulation of the breakdown of all three types of substrates, whose hydrolysis then resembled or exceeded that seen in untreated control proteasomes (Figure 6A). Thus, the aggregated species does not inactivate this Rpt5 gate opening mechanism, but reduces markedly its efficacy, most likely by helping maintain the closed state.

Aggregated β -sheet-rich PrP inhibits gate opening in 26S proteasomes stimulated by polyubiquitin conjugates

It has recently been reported that the binding of polyubiquitin-conjugated proteins to the 19S activator stimulates substrate hydrolysis by increasing gate opening in the 20S proteasome (Bech-Otschir *et al*, 2009; Peth *et al*, 2009). This mechanism appears to be important in enhancing the selectivity of the 26S proteasome for ubiquitinated proteins. To test whether β -sheet-rich PrP species are able to inhibit

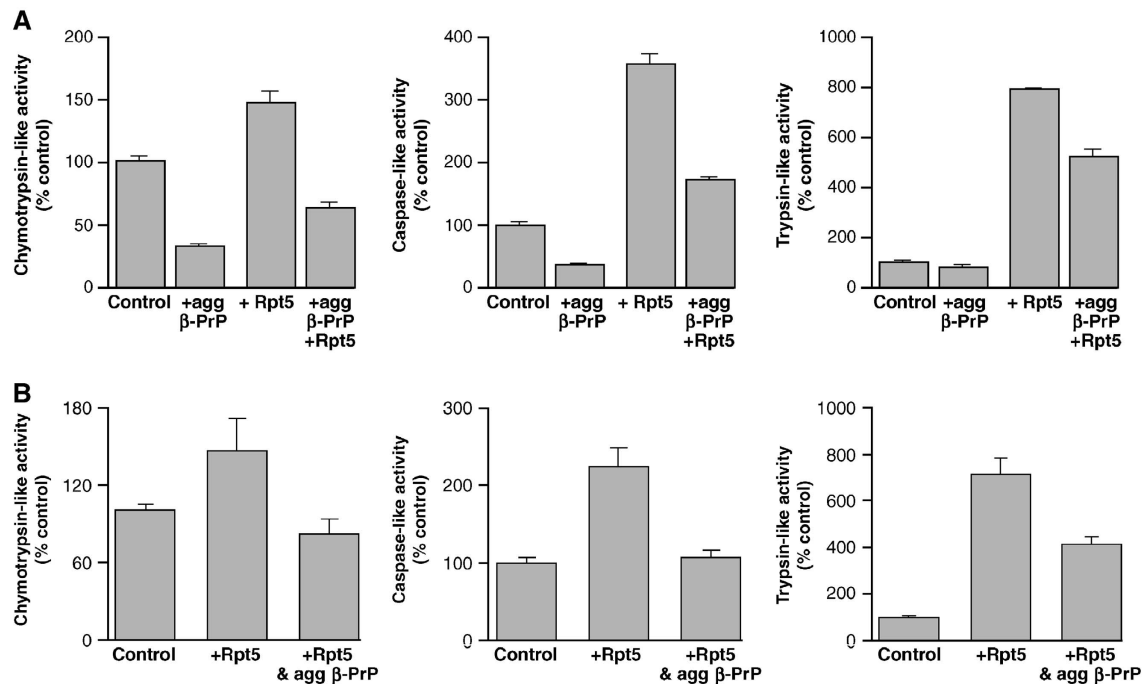


Figure 6 Rpt5-mediated gate opening in 20S proteasomes is decreased by β -sheet-rich PrP species. (A) Pre-incubating human 20S proteasomes with 50 μ g/ml aggregated β -PrP species before the addition of Rpt5 prevents Rpt5-mediated gate opening of the 20S ($P < 0.001$, versus respective Rpt5-activated 20S alone). (B) Incubating human 20S proteasomes with Rpt5 and 50 μ g/ml aggregated β -PrP at the same time results in inhibition of Rpt5-mediated gate opening in 20S (chymotrypsin $P < 0.01$, caspase and trypsin $P < 0.001$, versus respective Rpt5-activated 20S alone).

this induction of gate opening, they were incubated with affinity-purified 26S proteasomes in the presence of the E3 ligase, E6AP, which had either been allowed to autoubiquitinate by incubation with E1 and E2 ligases and ATP (Peth *et al*, 2009) (Ub-E6AP), or which remained in its unconjugated state as a control. As expected, only Ub-E6AP increased gate opening of the 26S proteasome, as assayed by its chymotrypsin-like activity, by approximately two-fold. However, the addition of aggregated β -PrP decreased the activity of the 26S to the basal (unstimulated) levels (Figure 7). Since the stimulation by Ub conjugates involves the ATPase C-termini (Peth *et al*, 2009), this clear inhibition of gate opening is in accord with the inhibition of gate opening in the 20S particle by Rpt5 peptides.

Aggregated β -sheet-rich PrP isoforms do not inhibit activation of 20S proteasomes by 11S regulators

Gate opening in the 20S proteasome can also be stimulated by a very different molecular mechanism by the 11S family of proteasome activators. PA26, the invertebrate 11S homologue of mammalian PA28, binds tightly to the ends of the 20S outer ring and stabilises the open-gate conformation (Whitby *et al*, 2000), but by a mechanism that is different to that of the ATPase subunits (Smith *et al*, 2007; Rabl *et al*, 2008). PA26 is a single subunit complex that can be easily expressed in an active homogenous form in *Escherichia coli* (Whitby *et al*, 2000; Yu *et al*, 2010), and the crystal structure of PA26 in a complex with the 20S particle and its mechanism of inducing gate opening are well defined (Whitby *et al*, 2000; Forster *et al*, 2005). If aggregated β -sheet-rich PrP isoforms bind similarly to the ends of the 20S particle to inhibit gate opening, then they should competitively inhibit the binding of 11S activators to the 20S proteasome. Therefore, their

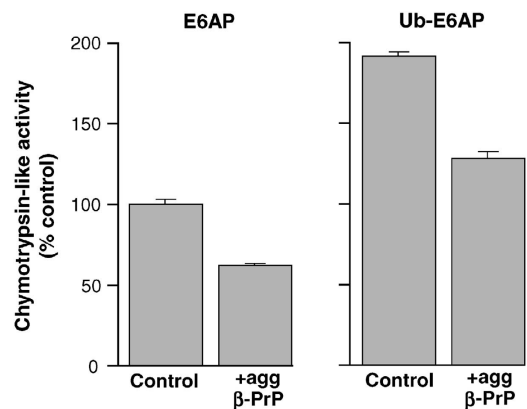


Figure 7 Gate opening in 26S proteasomes stimulated by polyubiquitinated conjugates is decreased by β -sheet-rich PrP species. Incubating rabbit 26S proteasomes with polyubiquitinated E6AP (Ub-E6AP) enhanced peptide hydrolysis (i.e., gate opening above levels with the non-ubiquitinated E6AP). Addition of 50 μ g/ml aggregated β -PrP results in inhibition of Ub-E6AP-mediated gate opening in 26S proteasomes ($P < 0.001$, versus respective E6AP-incubated 26S alone).

effects on PA26-activated proteasomes were tested. As expected, the recombinant PA26 caused a dramatic stimulation (> 20 -fold) of peptide hydrolysis by the 20S particles (Figure 8A). 20S proteasomes were incubated with both aggregated β -PrP and increasing concentrations of PA26 until a maximal stimulation of 20S was exceeded, indicating a saturation of the proteasomes' ends with PA26 complexes. Then peptide hydrolysis was monitored to assay gate opening. Although aggregated β -PrP by itself inhibited peptide hydrolysis by the three different sites in the 20S particle (also

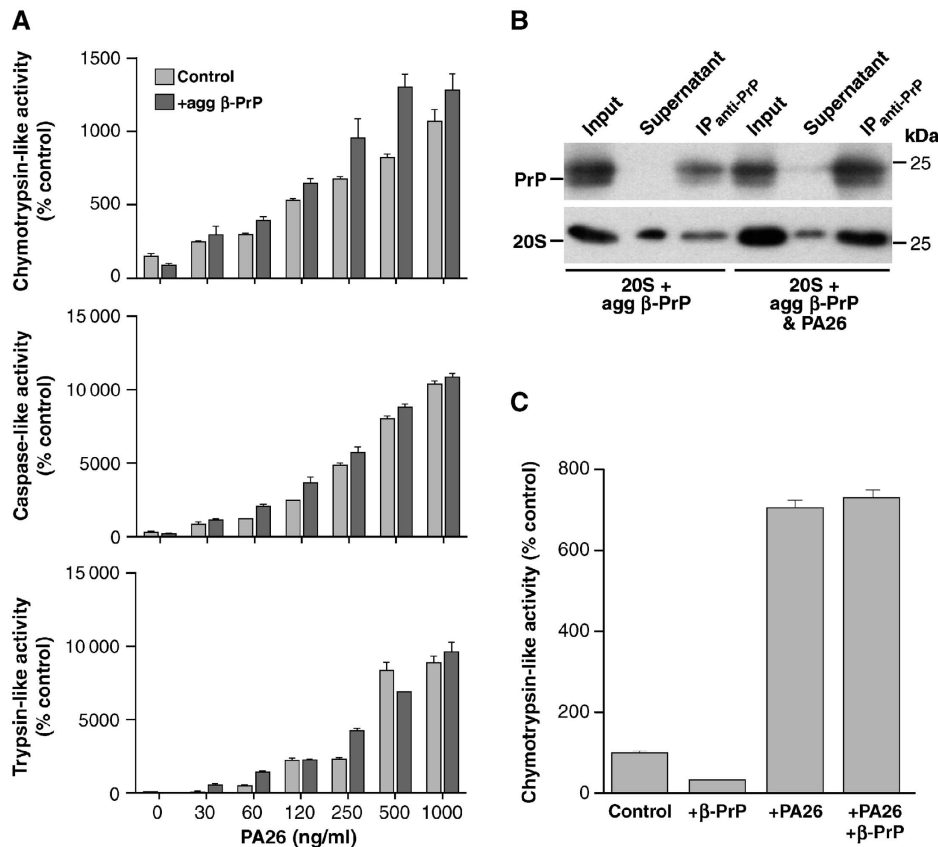


Figure 8 β -Sheet-rich PrP species bind to 20S proteasomes in the presence of PA26, but fail to inhibit PA26-mediated gate opening. (A) Incubating human 20S proteasomes with varying concentrations of PA26 (0–1 μ g/ml) and 50 μ g/ml aggregated β -PrP does not reveal any inhibition of PA26-mediated gate opening in the 20S. (B) Incubating human 20S proteasomes with 1 μ g/ml PA26 does not displace its binding by co-immunoprecipitation to aggregated β -PrP (50 μ g/ml). IP_{anti-PrP} and unbound (supernatant) fractions, together with input starting material, were immunoblotted with anti-PrP and anti-20S antibodies. (C) Aggregated β -PrP inhibits the control, but not PA26-stimulated 20S proteasomes used in the immunoprecipitation reaction mixtures.

see Figure 6A), it did not inhibit at all the PA26-activated 20S complex at any concentration of PA26 used (Figure 8A). In fact, in most experiments, the activity in the presence of aggregated β -PrP slightly exceeded that in its absence. By contrast, in parallel control experiments, the β -PrP still inhibited the gate opening induced by Rpt 5 C-terminal peptides (data not shown). Thus, the stimulating effects of PA26 dominate over and prevent gate closing by β -PrP aggregates, in sharp contrast with the gate opening mechanism of the 19S regulatory particle and its Rpt5 ATPase, which are susceptible to β -PrP inhibition.

The absence of any inhibition of PA26-activated proteasomes led us to reinvestigate the effect of aggregated β -PrP on PA28-activated proteasomes, as has previously been described (Kristiansen *et al*, 2007). The 20S particles were incubated with aggregated β -PrP and with increasing concentrations of purified PA28 α/β , and then peptide hydrolysis was monitored to assay gate opening. However, the preparation of purified PA28 used previously (obtained from the same commercial source and used at the same concentrations) did not induce gate opening (Supplementary Figure S4A). At very high concentrations of PA28 α/β (as high as was achievable), some small stimulation of gate opening above control levels was seen, but surprisingly, no inhibitory effect of aggregated β -PrP was observed. Aggregated β -PrP inhibited peptide hydrolysis only at concentrations of PA28 α/β that

failed by themselves to cause any activation (Supplementary Figure S4A) (as was seen in the absence of PA28 α/β). We conclude, therefore, that our earlier observations suggesting that β -PrP could inhibit PA28-activated proteasomes were obtained with preparations of PA28 α/β that were inactive at the concentrations used. To obtain a clearer answer, therefore, as to whether or not aggregated β -PrP can inhibit proteasomes activated by PA28, similar experiments were carried out with recombinant PA28 α , which unlike the prior preparation stimulated gate opening dramatically (Supplementary Figure S4B). The resulting peptide hydrolysis by the PA28-activated 20S complex was not inhibited at all by aggregated β -PrP at any concentration of PA28 α used (Supplementary Figure S4B), in accord with the results obtained with PA26 (Figure 8A).

Aggregated β -sheet-rich PrP and PA26 do not bind to the same site on the 20S proteasome

Because aggregated β -PrP did not inhibit PA26-activated 20S particles at any concentration of PA26 used, it is unlikely that PA26 competes with the PrP aggregates for binding to the 20S proteasome. To confirm this conclusion, we did a pull-down experiment to determine whether aggregated β -PrP, the 20S proteasome and PA26 were all found in one complex, and whether saturating amounts of PA26 decrease β -PrP binding to the 20S. Therefore, we used anti-PrP Ab-coated beads to

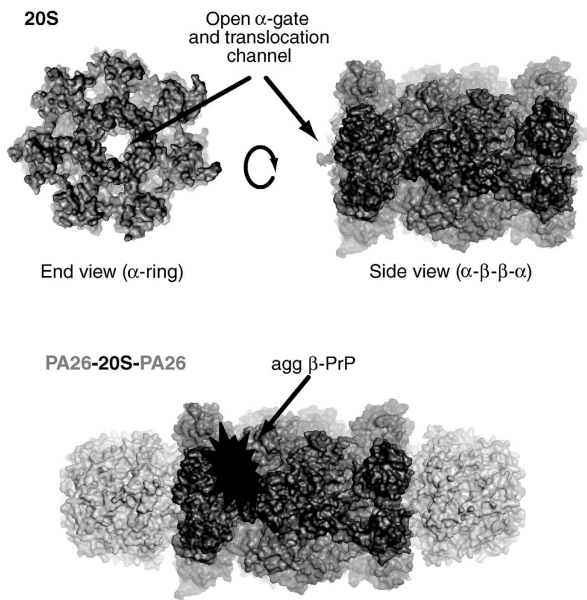


Figure 9 Schematic model proposing the location of aggregated β -PrP binding to the 20S proteasome. Since aggregated β -PrP species do not inhibit open-gated mutant 20S proteasomes ($\alpha 3\Delta N$), and because they remain bound to the 20S even in the presence of saturating concentrations of PA26 (which completely occludes the ends of the 20S), this indicates that they do not inhibit the 20S proteasome either by entering the degradation chamber or by binding at the end surface of the 20S α -ring to block substrate entry or affect gate opening. Therefore, the most likely site of binding is the outer lateral surface of the 20S particle, where PA26 does not bind. Since the aggregated β -PrP inhibits gate opening to block proteasome function, it most likely makes contact with the lateral side of the 20S α -subunits, as shown.

test if the 20S particles could still be co-immunoprecipitated in the presence of a saturating concentration of PA26. Figure 8B shows that β -PrP was co-immunoprecipitated with 20S proteasomes even when they were bound at both ends to PA26 (i.e., when saturated; Figure 8B). PA26 was also present in the PrP precipitates (Supplementary Figure S5A). Thus, PA26 does not block the association of prions with the 20S particle and, in fact, even more proteasomes appeared to be associated with β -PrP in the presence of PA26. Additional assays confirmed that under these conditions, the 20S particle was strongly activated by PA26, and β -PrP did not reduce its activity in the presence of PA26 (Figure 8C). In similar experiments, in which a saturating concentration of the Rpt5 peptide was used, there was also no reduction in the amount of 20S proteasomes that co-immunoprecipitated with aggregated β -PrP in the presence of Rpt5 (Supplementary Figure S5B), as was seen with PA26. Since aggregated β -sheet-rich PrP and PA26 are able to bind to the 20S particle at the same time, and since PA26 binds on top of the α -ring, these data imply that the PrP does not bind to this surface, and therefore, probably associates with the 20S particle's cylindrical walls (see Figure 9 for schematic cartoon).

Discussion

The present studies have uncovered a novel mechanism for inhibition of proteasome function that appears to contribute to the pathogenesis of prion disease. We previously found that prion infection impairs protein degradation by the UPS in

mouse brain and cultured neurons by inhibiting the function of the 26S proteasome (Kristiansen *et al*, 2007). However, the exact mechanism by which β -sheet rich PrP isoforms reduce proteasome activity was unknown. Here, we demonstrate that disease-associated aggregated β -sheet-rich forms of PrP impair protein degradation by inhibiting gate opening and substrate entry into the 20S particle. Accordingly, β -sheet-rich PrP species were found to decrease hydrolysis of various peptides and proteins by purified yeast and human 20S proteasomes, but did not inhibit yeast open-gated mutant 20S ($\alpha 3\Delta N$) particles. Furthermore, β -sheet-rich PrP species bind to, but fail to inhibit, open-gated mutant 26S proteasomes and the PA26-20S complex, in contrast to the inhibitory effect on wild-type 26S particles.

When 20S proteasomes are in a latent (non-activated) state, the gate is formed by interactions of the N-terminal tails of its seven α -subunits (Groll *et al*, 2000). In 26S proteasomes, the 19S ATPases regulate the opening of this entry channel, but several other regulatory factors (PA200, PA28 or, in certain invertebrates, PA26) are known to activate the 20S particle by causing gate opening by distinct ATP-independent mechanisms. In addition, when ubiquitinated proteins bind to 26S particles, the substrate entry channel is opened further to fully activate the degradation of ubiquitinated substrates (Bech-Otschir *et al*, 2009; Li and DeMartino, 2009; Peth *et al*, 2009). The structural backbone of the 20S proteasome gate is provided by the N-terminus of the 20S's $\alpha 3$ -subunit, and its deletion in the $\alpha 3\Delta N$ mutant prevents formation of the closed-gate conformation, leaving the proteasomes in a continually activated (open-gated) form (Groll *et al*, 2000). Since aggregated β -sheet-rich PrP can bind to, but cannot inhibit open-gated $\alpha 3\Delta N$ particles, or 20S-PA26 complexes in which the gate is buried and inaccessible (Whitby *et al*, 2000; Forster *et al*, 2005), these β -PrP species cannot be binding directly to the gate, but must act indirectly and allosterically to stabilise its closed form (e.g., as proposed in Figure 9). By contrast, if the β -PrP aggregates were able to traverse the narrow pore into the 20S particle, which is sterically highly unlikely, and to directly inhibit the active sites located within its central chamber, then the magnitude of the inhibition of peptide hydrolysis would be equal to or greater in the $\alpha 3\Delta N$ mutant 20S proteasomes than in wild-type particles. However, the exact opposite results were observed.

Another observation consistent with an effect on gating was that β -PrP aggregates caused greater inhibition of the hydrolysis of substrates by the chymotrypsin-like and caspase-like sites than by the trypsin-like site, whose rate of hydrolysis (under typical substrate concentrations) is limited primarily by slow turnover rate of this active site rather than by substrate entry (Kisselev *et al*, 2002). Accordingly, treatments that promote gate opening (e.g., the $\alpha 3\Delta N$ deletion) or inhibit it (e.g., incubation with intracellular levels of KCl) also have smaller relative effects on the trypsin-like activity. This novel mechanism of inhibition by aggregated β -sheet-rich PrP species at the level of gate opening contrasts sharply with that of the proteasome inhibitors widely used as research tools and in the clinic for treatment of haematological malignancies, all of which bind to the peptidase sites, particularly the chymotrypsin-like site (Kisselev and Goldberg, 2001).

During proteolysis, the 19S complex carries out multiple ATP-dependent processes resulting in the translocation of a

polypeptide through the gated entry channel into the 20S particle (Pickart and Cohen, 2004; Peth *et al*, 2009). When the 19S ATPases bind a nucleotide, their conserved C-terminal HbYX motifs dock into the pockets between the adjacent α -subunits, functioning like a 'key in a lock' to destabilise the closed conformation and open the gate (Smith *et al*, 2007; Rabl *et al*, 2008). Peptides that correspond to these C-termini, such as the Rpt5 used here, function similarly to induce gate opening (Smith *et al*, 2007; Gillette *et al*, 2008). Structural analyses of the homologous complex from archaea indicate that the HbYX residues interact with conserved residues in the 20S proteasome, triggering a rotation of the α -subunits to cause gate opening (Rabl *et al*, 2008; Yu *et al*, 2010). By themselves, these C-terminal peptides have relatively low affinities for the intersubunit pockets, and therefore under these *in vitro* conditions must be continually binding and dissociating, leading to a continual opening and closing of the gate. This weak binding can explain why a similar inhibition of gate opening was observed irrespective of whether the β -PrP species were added before or after activation of the 20S particle with Rpt5.

Though the β -sheet-rich PrP aggregates reduced the extent of gate opening with Rpt5, it should be noted that in the presence of the aggregated β -PrP, the Rpt5 peptide still enhanced gate opening several fold. Thus, while β -PrP favours the closed state, the Rpt5 peptide promotes gate opening, and when both are present, a partial gate opening response was observed. A similar partial inhibition of gate opening was observed with 26S proteasomes, in which gate opening was stimulated by the addition of a polyubiquitin-conjugated protein. In addition to targeting protein to the 26S complex, ubiquitin conjugates (e.g., the ubiquitinated E6AP used here) have been shown to bind to the Usp14 subunit of the 19S regulator to enhance gate opening and substrate hydrolysis (Bech-Otschir *et al*, 2009; Peth *et al*, 2009). Thus, polyubiquitinated substrates appear to activate the proteasome and to allosterically stimulate their own degradation, a step coupled to the disassembly of the ubiquitin chain by the Usp14 (Peth *et al*, 2009). Although β -sheet-rich PrP aggregates clearly reduce the extent of gate opening induced by polyubiquitin conjugates, the polyubiquitin was still able to induce further gate opening in the presence of aggregated β -PrP, as was also observed using 20S proteasomes and the Rpt5 peptide.

It is especially intriguing that while aggregated β -sheet-rich PrP decreases basal, Rpt5-stimulated 20S and polyubiquitin-stimulated 26S activities, the PrP does not inhibit the activation of the 20S by PA26 or PA28. Although both 11S regulators and the proteasome regulatory ATPases (e.g., Rpt5) associate with the 20S particle via docking of their C-termini into the α -ring pockets, they stimulate gate opening by distinct mechanisms (Whitby *et al*, 2000; Forster *et al*, 2005; Rabl *et al*, 2008; Yu *et al*, 2010). Gate opening by PA26 also requires a separate activation domain, which pushes on the base of the gating residues, destabilising the closed conformation and stabilising the open gate. Interestingly, this mechanism involves only a small (~ 1.5 Å) shift of Pro17 upon PA26 binding and does not require large conformational changes in the α -ring (Forster *et al*, 2005). In contrast, binding of the 19S ATPases' C-termini or peptides containing a HbYX motif by themselves induce a 4° rotation of the entire α -subunits to reposition the critical Pro17 so as to destabilise the closed

form and cause gate opening. Since aggregated β -sheet-rich PrP inhibits basal and Rpt5-activated 20S proteasomes, and the 26S proteasome, but not the 20S-PA26 (or 20S-PA28) complex, they probably act by stabilising the 'un-rotated' (closed-gate) subunit conformation. Such an effect would reduce gate opening and proteolysis induced by the C-termini of the ATPases, but not by PA26, which induces gate opening without α -subunit rotation. Latent 20S particles, when gently isolated, are normally in the closed-gate conformation at 37°C , but they exhibit a low level of peptidase activity due to a spontaneous basal rate of gate opening in which the 20S gate is constantly fluctuating between open and closed states (Osmulski *et al*, 2009). Therefore, binding of aggregated β -PrP species to the 20S particle presumably inhibits this spontaneous opening to reduce basal activity by stabilising the closed ('un-rotated') form of the α -subunits.

These results raise the obvious question—how does the aggregated β -PrP species bind to and inhibit the 20S proteasome? Our data show that aggregated β -sheet-rich PrP remains bound to the 20S proteasome in the presence of saturating concentrations of PA26, even though it does not inhibit this PA26-20S complex. Given that the β -sheet-rich PrP aggregates are far too large to enter the narrow 13 Å channel of the proteasome, and that PA26 binds tightly to both ends of the 20S barrel, then by exclusion the β -PrP aggregates must bind to the outer lateral surface of the 20S (as suggested in Figure 9). This model is also consistent with our prior observations that these relatively large β -sheet-rich PrP aggregates inhibit the 26S proteasome without displacing the 19S regulatory particles (Kristiansen *et al*, 2007), which bind to the same ends of the 20S particle as PA26. Binding to the outer surface is compatible with a mechanism in which aggregated β -PrP inhibits gate opening by the 19S ATPases by interfering with α -subunit rotation (Rabl *et al*, 2008; Yu *et al*, 2010), but cannot inhibit gate opening by PA26, which uses an activation loop to affect the gate directly without causing subunit rotation. The lateral surface of the 20S particle has deep crevices and pockets that could certainly act as potential binding sites, and association with the lateral surface near the α -ring is the most plausible location where the β -sheet-rich aggregates could inhibit gate opening by the 19S complex without displacing it from the 20S particle (Figure 9).

In other protein-misfolding neurodegenerative disorders, there is evidence that soluble oligomeric aggregates, rather than large insoluble aggregates, are the disease-causing protein species (Caughey and Lansbury, 2003; Haass and Selkoe, 2007). Indeed, subclinical models of prion infection, where extracellular prion amyloid plaques accumulate but do not cause disease (Hill *et al*, 2000), suggest that prion neurotoxicity is not due to extracellular PrP^{Sc} *per se*, but due to the accumulation of cellular oligomeric intermediates produced during prion conversion or breakdown of PrP^{Sc} (Collinge and Clarke, 2007). Structural studies of recombinant PrP have shown that its protease-resistant core can fold into both amyloid fibrils and β -sheet-rich oligomers (Baskakov *et al*, 2002; Sokolowski *et al*, 2003), but the sizes of such β -oligomers remain poorly defined (Martins *et al*, 2006; Gerber *et al*, 2007). Moreover, unlike aggregated β -sheet-rich PrP, PrP amyloid fibrils do not inhibit the 26S proteasome (Kristiansen *et al*, 2007). The current observations also support the notion that the inhibitory species is small, although structural characterisation at this stage is not possible due to

the highly insoluble and heterogeneous nature of PrP aggregates. When yeast 20S proteasomes were incubated with increasing amounts of aggregated β -sheet-rich PrP, the apparent IC_{50} was between 90 and 180 nM (monomeric concentration), which corresponds to a molar ratio of 10–20 PrP monomers per 20S proteasome in the solution. Although the mean number of monomers per β -PrP aggregate is unknown, the aggregates of β -PrP must be present at much lower concentrations approaching that of the 20S particle in these experiments and must, therefore, have a high affinity for the proteasome.

Several prior observations indicate a large impairment of protein degradation by the UPS in prion-infected cells and mouse brain (Kristiansen *et al*, 2007). Recent findings that transgenic mice expressing mutant, albeit non-infectious (Chiesa *et al*, 2003), forms of PrP associated with certain inherited human prion diseases do not show UPS impairment (Quaglio *et al*, 2011), contrast with the clear accumulation of ubiquitinated proteins and reporter substrates indicating UPS dysfunction when cells or animals are inoculated with infectious prions (Kang *et al* 2004, Kristiansen *et al* 2007). Differences may also be accounted for by acute versus chronic expression of mutant proteins, and their aggregation status, as found recently in cellular and transgenic models of HD (Ortega *et al*, 2010). Furthermore, we found here that aggregated β -sheet-rich PrP impairs 20S-mediated degradation of FITC-labelled casein *in vitro*, and causes accumulation of several specific short-lived UPS substrates *in vivo*, including I κ B α (Alkalay *et al*, 1995), p27 (Pagano *et al*, 1995) and p53 (Ciechanover, 1994). The accumulation of such critical short-lived regulators of fundamental cellular processes (Toyoshima and Hunter, 1994; Perkins and Gilmore, 2006) could lead to impairment of neuronal function and contribute to neurotoxicity. In this regard, the accumulation of I κ B α could be particularly important since it normally inhibits NF- κ B activation. Furthermore, increased levels of p27 in prion-infected brain could lead to cell-cycle arrest by binding cyclin and Cdk molecules and, in fact, proteasome inhibitors are known to arrest cell proliferation in part by increasing p21 and p27 levels (Baiz *et al*, 2009). Similarly, as p53 is a key regulator of apoptosis in response to DNA damage (Levine, 1997), its accumulation in neural cells could also have detrimental consequences.

Here, we present evidence that prion disease-associated aggregated β -sheet-rich PrP species inhibit the proteasome by decreasing gate opening in the 20S particle. We also demonstrate that PrP isoforms directly interact with the 26S proteasome both *in vitro* and *in vivo*, and cause an accumulation of key UPS substrates in prion-infected mouse brains. Our findings, moreover, may have relevance beyond prion diseases. For example, in AD, similar *in vitro* studies have demonstrated a direct binding of amyloid β -protein (A β) to bovine 20S proteasomes resulting in a reduction in chymotrypsin-like activity (Gregori *et al* 1995, 1997). Furthermore, AD transgenic mice show impaired proteasome activity that correlates with an accumulation of intraneuronal A β oligomers (Tseng *et al*, 2008), but the precise mechanisms underlying these observations remain unknown. Our findings, therefore, serve as a model for understanding how misfolded β -sheet-rich proteins may impair proteasome function in other neurodegenerative diseases that are also characterised by the accumulation of such protein species.

Materials and methods

Reagents

Human 26S and 20S proteasomes, Suc-LLVY-amc, Boc-LRR-amc and PA28 were from Enzo Life Sciences. Ac-nLPnLD-amc and Z-GGL-amc were from Bachem, and recombinant PA28 α was from Abcam. Rpt5 peptides were synthesised by EZBiolabs. PA26 was synthesised in B121 cells and purified by affinity with a Ni-NTA column, as described (Yu *et al*, 2010). Wild-type yeast 20S proteasomes were purified from the EUROSCAF *Saccharomyces cerevisiae* wild-type strain BY4741 (*MAT α his3- Δ 1, leu2- Δ 0, met15- Δ 0, ura3- Δ 0*), as described (Bajorek *et al*, 2003). The α 3 Δ N yeast 20S mutant proteasomes were a kind gift from Dr Alexei Kisselev, Dartmouth Medical School, USA; wild-type and α 3 Δ N yeast 26S proteasomes were from Dr Andreas Peth, Harvard Medical School, USA. Rabbit 26S proteasomes were isolated by affinity purification, as described (Besche *et al*, 2009). Ubiquitin conjugates were prepared by allowing the ubiquitin ligase, E6AP, to autoubiquitinate. GST-tagged E6AP, expressed in *E. coli*, was incubated with E1, UbCH5 as the E2 and ATP, and the conjugates were eluted with 5 mM glutathione, as previously described (Peth *et al*, 2009). Murine recombinant PrP in either the oxidised (α -PrP) or reduced (β -PrP) form was prepared and aggregated as described (Jackson *et al*, 1999a,b; Kristiansen *et al*, 2007). PrP^{Sc} was semi-purified from RML-infected GT-1 cells (Kristiansen *et al*, 2007).

Assaying proteasome activity with fluorogenic substrates

Unless otherwise specified, human 26S (0.4 nM) or 20S (1.4 nM) proteasomes were assayed using fluorogenic peptides, as described previously (Kristiansen *et al*, 2007). Briefly, proteasomes were incubated in a reaction buffer containing 50 mM Tris-HCl (pH 7.4), 1 mM DTT and 100 μ M fluorogenic substrate (Suc-LLVY-amc, Ac-nLPnLD-amc or Boc-LRR-amc). Human 20S proteasomes were activated with 250 μ M Rpt5, or with PA28 or PA26 as indicated. Yeast wild-type and α 3 Δ N 20S particles were used at 9 nM for yeast proteasome assays. Yeast wild-type and α 3 Δ N, and human 26S proteasomes were used at 0.4 nM in the presence of 2 mM ATP and 10 mM MgCl₂. Rabbit 26S proteasomes were used at 5 nM in 25 mM HEPES (pH 7.5), 2.5 mM MgCl₂, 125 mM CH₃CO₂K, 0.05% Triton X-100, 0.1 μ g/ml BSA, 0.5 mM DTT, 0.5 mM ATP and 10 μ M fluorogenic substrate (Z-GGL-amc). Fluorescence was measured every 30 s for 45 min ($\lambda_{ex}/\lambda_{em}$ = 360:460).

Casein degradation by yeast 20S proteasomes

Wild-type yeast 20S proteasomes (0.6 μ M) were incubated with varying amounts of aggregated β -PrP or aggregated α -PrP for 1 h at 30°C. HiLyteTM-488 casein conjugate was then added to each reaction (AnaSpec). Fluorescence was measured every 5 min ($\lambda_{ex}/\lambda_{em}$ = 492:535).

Co-immunoprecipitation

RML mouse prions were propagated in CD1 mice, which were culled when terminally sick. Whole brains were homogenised in PBS as described (Kristiansen *et al*, 2005), diluted to 1 mg/ml in PBS/1% Tween-20 (PBS-T) and incubated for 20 min on ice. Debris was removed by centrifugation at 2000 g (2 min). The supernatant (500 μ g; starting material) was incubated overnight with 40 μ l magnetic tosyl-activated beads (Invitrogen) coated with either mouse monoclonal antibody to PrP (ICSM35; D-GEN), rabbit polyclonal antibody to the 'core' 20S subunits, or with BSA alone as a control, as per the manufacturer's instructions. The beads were isolated using a DynaMag magnet (Invitrogen), which allows the removal of the unbound fraction (supernatant), and washed four times with PBS-T before being resuspended and boiled in SDS sample buffer (IP fraction). In similar experiments, human 20S proteasomes (0.1 μ M) were incubated with 30 μ g/ml aggregated β -PrP or 30 μ g/ml aggregated α -PrP in 50 mM Tris-HCl (pH 7.4), 1 mM DTT for 1 h at 37°C. The samples were then incubated with either ICSM35-coated or control BSA-coated beads overnight and the beads were then isolated and washed as described above. Further experiments were performed using human 26S, wild-type or α 3 Δ N yeast 26S proteasomes in 50 mM Tris-HCl (pH 7.4), 1 mM DTT, 10 mM MgCl₂ and 2 mM ATP. Immunoblotting was conducted on starting material (input), unbound (supernatant) and IP fractions, using rabbit polyclonal anti-20S (Enzo Life Sciences; recognises α_5/α_7 , β_1 , β_5 , β_{5i} , β_7) and ICSM35 anti-PrP antibodies.

PrP was analysed by immunoblotting the IP fraction either directly or after PK digestion (5 µg/ml PK for 45 min at 37°C). 19S components Rpt1 and Rpn7 were detected using specific monoclonal and polyclonal antibodies, respectively (Enzo Life Sciences).

SDS-PAGE and immunoblotting

Whole brains from terminally-ill RML-infected mice (CD1 for IκBα and p27; C57BL/6 for p53) were homogenised and electrophoresed as described (Kristiansen *et al*, 2005), blotting with a rabbit polyclonal anti-IκBα antibody (Santa Cruz; 1:1000), a mouse monoclonal anti-p27 antibody (F-8 clone, Santa Cruz; 1:200) or a mouse monoclonal anti-p53 antibody (Cell Signaling Technology; 1:1000). Densitometry was performed using the Kodak Digital Science™ Image station 440CF (IS440CF) system and analysed using the Kodak ID Image Analysis Software (Perkin-Elmer Life Sciences).

Quantitative PCR

RNA was isolated from whole brains from uninfected or RML prion-infected end-stage mice using TRIzol (Invitrogen). Total RNA was reverse transcribed using Superscript II Reverse Transcriptase and random primers (Invitrogen). *Iκba*, *P27* and *P53* real-time PCR was performed using 1 µl cDNA on a 7500 Fast Real-time PCR System (ABI). ROX MegaMixGold (Microzone) was used for *Iκba* and SYBR Green (ABI) for *P27* and *P53*. Transcript-specific primers were used for *Iκba* (forward 5'-ACCTGCACACCCAGCAT-3', reverse 5'-CGTGTGGCCATTGTAGTTGGT-3', probe 5'-TCCACTCCGTCCTGC-3'); *P27* (forward 5'-GTGGACAAATGCCTGACTC-3', reverse 5'-TTCGGA GCTGTTTACGTC-3'); and *P53* (forward 5'-GCGTAAACGCTTCGA GATGTT-3', reverse 5'-TTTTTATGGCGGAAGTAGACTG-3'). Mouse β-actin was used as an endogenous control. The relative amount of specifically amplified cDNA was calculated from standard curves using the comparative threshold cycle method.

References

Alkalay I, Yaron A, Hatzubai A, Orian A, Ciechanover A, Benveniste Y (1995) Stimulation-dependent I-kappa-B-alpha phosphorylation marks the Nf-kappa-B inhibitor for degradation via the ubiquitin-pathway. *Proc Natl Acad Sci USA* **92**: 10599–10603

Baiz D, Pozzato G, Dapas B, Farra R, Scaggiante B, Grassi M, Uxa L, Giansante C, Zennaro C, Guarnieri G, Grassi G (2009) Bortezomib arrests the proliferation of hepatocellular carcinoma cells HepG2 and JHH6 by differentially affecting E2F1 p21 and p27 levels. *Biochimie* **91**: 373–382

Bajorek M, Finley D, Glickman MH (2003) Proteasome disassembly and downregulation is correlated with viability during stationary phase. *Curr Biol* **13**: 1140–1144

Baskakov IV, Legname G, Baldwin MA, Prusiner SB, Cohen FE (2002) Pathway complexity of prion protein assembly into amyloid. *J Biol Chem* **277**: 21140–21148

Bech-Otschir D, Helfrich A, Enenkel C, Consiglieri G, Seegar M, Holzhütter HG, Dahlmann B, Kloetzel PM (2009) Polyubiquitin substrates allosterically activate their own degradation by the 26S proteasome. *Nat Struct Mol Biol* **16**: 219–225

Bedford L, Hay D, Devoy A, Paine S, Powe DG, Seth R, Gray T, Topham I, Fone K, Rezvani N, Mee M, Soane T, Layfield R, Sheppard PW, Ebendal T, Usoskin D, Lowe J, Mayer RJ (2008) Depletion of 26S proteasomes in mouse brain neurons causes neurodegeneration and Lewy-like inclusions resembling human pale bodies. *J Neurosci* **28**: 8189–8198

Besche HC, Haas W, Gygi SP, Goldberg AL (2009) Isolation of mammalian 26S proteasomes and p97/VCP complexes using the ubiquitin-like domain from HHR23B reveals novel proteasome-associated proteins. *Biochemistry* **48**: 2538–2549

Bueler H, Aguzzi A, Sailer A, Greiner RA, Autenried P, Aguet M, Weissmann C (1993) Mice devoid of PrP are resistant to scrapie. *Cell* **73**: 1339–1347

Caughy B, Baron GS (2006) Prions and their partners in crime. *Nature* **443**: 803–810

Caughy B, Lansbury PT (2003) Protofibrils, pores, fibrils and neurodegeneration: separating the responsible protein aggregates from the innocent bystanders. *Annu Rev Neurosci* **26**: 267–298

Chiesa R, Piccardo P, Quaglio E, Drisaldi B, Si-Hoe SL, Takao M, Ghetti B, Harris DA (2003) Molecular distinction between patho-

Statistical analysis

Data are expressed as mean ± s.e.m. of at least three experiments, unless stated otherwise. Data containing two groups were analysed using an unpaired Student's *t*-test; groups of three or more were analysed by one-way analysis of variance with Tukey–Kramer *post hoc* tests. For all statistical analyses, a value of *P* < 0.05 was considered significant.

Supplementary data

Supplementary data are available at *The EMBO Journal* Online (<http://www.embojournal.org>).

Acknowledgements

We thank Graham Jackson, Anthony Clarke, Clare Trevitt and members of the MRC Prion Unit for experimental suggestions and advice; Mark Batchelor for preparing recombinant prion proteins; and Ray Young for graphics. This work was funded by grants to SJT from the Medical Research Council and UK Department of Health and to ALG from the NIH (NIGMS 5 R01 GM51923-13), the Multiple Myeloma Foundation and Johnson and Johnson, Inc. PD was the recipient of a Brain Research Trust Studentship.

Author contributions: SJT conceived and supervised the study. PD, RA and SJT drafted the manuscript. PD, RA, RG, KJK, MK, JAN, RR and DK performed the experiments. PD, RA, DMS, MHG, JC, ALG and SJT contributed to study design, data analysis and interpretation of results. All authors commented on the final manuscript text.

Conflict of interest

The authors declare that they have no conflict of interest.

genic and infectious properties of the prion protein. *J Virol* **77**: 7611–7622

Ciechanover A (1994) The ubiquitin-proteasome proteolytic pathway. *Cell* **79**: 13–21

Collinge J, Clarke AR (2007) A general model of prion strains and their pathogenicity. *Science* **318**: 930–936

Deriziotis P, Tabrizi SJ (2008) Prions and the proteasome. *Biochim Biophys Acta* **1782**: 713–722

Forster A, Masters EI, Whitby FG, Robinson H, Hill CP (2005) The 19 A structure of a proteasome-11S activator complex and implications for proteasome-PAN/PA700 interactions. *Mol Cell* **18**: 589–599

Gerber R, Tahiri-Alaoui A, Hore PJ, James W (2007) Oligomerization of the human prion protein proceeds via a molten globule intermediate. *J Biol Chem* **282**: 6300–6307

Gillette TG, Kumar B, Thompson D, Slaughter CA, DeMartino GN (2008) Differential roles of the COOH termini of AAA subunits of PA700 (19 S regulator) in asymmetric assembly and activation of the 26 S proteasome. *J Biol Chem* **283**: 31813–31822

Glickman MH, Ciechanover A (2002) The ubiquitin-proteasome proteolytic pathway: destruction for the sake of construction. *Physiol Rev* **82**: 373–428

Goldberg AL (2003) Protein degradation and protection against misfolded or damaged proteins. *Nature* **426**: 895–899

Gregori L, Fuchs C, Figueiredo-Pereira ME, Van Nostrand WE, Goldgaber D (1995) Amyloid beta-protein inhibits ubiquitin-dependent protein degradation *in vitro*. *J Biol Chem* **270**: 19702–19708

Gregori L, Hainfeld JF, Simon MN, Goldgaber D (1997) Binding of amyloid beta protein to the 20S proteasome. *J Biol Chem* **272**: 58–62

Groll M, Bajorek M, Kohler A, Moroder L, Rubin DM, Huber R, Glickman MH, Finley D (2000) A gated channel into the proteasome core particle. *Nat Struct Biol* **7**: 1062–1067

Haass C, Selkoe DJ (2007) Soluble protein oligomers in neurodegeneration: lessons from the Alzheimer's amyloid beta-peptide. *Nat Rev Mol Cell Biol* **8**: 101–112

Hill AF, Joiner S, Linehan J, Desbruslais M, Lantos PL, Collinge J (2000) Species-barrier-independent prion replication in

- apparently resistant species. *Proc Natl Acad Sci USA* **97**: 10248–10253
- Jackson GS, Hill AF, Joseph C, Hosszu L, Power A, Waltho JP, Clarke AR, Collinge J (1999a) Multiple folding pathways for heterologously expressed human prion protein. *Biochim Biophys Acta* **1431**: 1–13
- Jackson GS, Hosszu LL, Power A, Hill AF, Kenney J, Saibil H, Craven CJ, Waltho JP, Clarke AR, Collinge J (1999b) Reversible conversion of monomeric human prion protein between native and fibrillogenic conformations. *Science* **283**: 1935–1937
- Kang SC, Brown DR, Whiteman M, Li R, Pan T, Perry G, Wisniewski T, Sy MS, Wong BS (2004) Prion protein is ubiquitinated after developing protease resistance in the brains of scrapie-infected mice. *J Pathol* **203**: 603–608
- Kisselev AF, Akopian TN, Woo KM, Goldberg AL (1999) The sizes of peptides generated from protein by mammalian 26 and 20 S proteasomes. Implications for understanding the degradative mechanism and antigen presentation. *J Biol Chem* **274**: 3363–3371
- Kisselev AF, Callard A, Goldberg AL (2006) Importance of the different proteolytic sites of the proteasome and the efficacy of inhibitors varies with the protein substrate. *J Biol Chem* **281**: 8582–8590
- Kisselev AF, Goldberg AL (2001) Proteasome inhibitors: from research tools to drug candidates. *Chem Biol* **8**: 739–758
- Kisselev AF, Kaganovich D, Goldberg AL (2002) Binding of hydrophobic peptides to several non-catalytic sites promotes peptide hydrolysis by all active sites of 20 S proteasomes. Evidence for peptide-induced channel opening in the alpha-rings. *J Biol Chem* **277**: 22260–22270
- Kohler A, Cascio P, Leggett DS, Woo KM, Goldberg AL, Finley D (2001) The axial channel of the proteasome core particle is gated by the Rpt2 ATPase and controls both substrate entry and product release. *Mol Cell* **7**: 1143–1152
- Kristiansen M, Deriziotis P, Dimcheff DE, Jackson GS, Ovaas H, Naumann H, Clarke A, van Leeuwen FW, Menendez-Benito V, Dantuma NP, Portis JL, Collinge J, Tabrizi SJ (2007) Disease-associated prion protein oligomers inhibit the 26S proteasome. *Mol Cell* **26**: 175–188
- Kristiansen M, Messenger SJ, Klohn PC, Brandner S, Wadsworth JD, Collinge J, Tabrizi SJ (2005) Disease-related prion protein forms aggregates in neuronal cells leading to caspase activation and apoptosis. *J Biol Chem* **280**: 38851–38861
- Levine AJ (1997) p53, the cellular gate keeper for growth and division. *Cell* **88**: 323–331
- Li X, DeMartino GN (2009) Variably modulated gating of the 26S proteasome by ATP and polyubiquitin. *Biochem J* **421**: 397–404
- Lindsten K, Menendez-Benito V, Masucci MG, Dantuma NP (2003) A transgenic mouse model of the ubiquitin/proteasome system. *Nat Biotechnol* **21**: 897–902
- Lloyd SE, Maytham EG, Pota H, Grizenkova J, Molou E, Uphill J, Hummerich H, Whitfield J, Alpers MP, Mead S, Collinge J (2009) HECTD2 is associated with susceptibility to mouse and human prion disease. *PLoS Genet* **5**: e1000383
- Mallucci GR, Rattie S, Asante EA, Linehan J, Gowland I, Jefferys JG, Collinge J (2002) Post-natal knockout of prion protein alters hippocampal CA1 properties but does not result in neurodegeneration. *EMBO J* **21**: 202–210
- Martins SM, Frosoni DJ, Martinez AM, De Felice FG, Ferreira ST (2006) Formation of soluble oligomers and amyloid fibrils with physical properties of the scrapie isoform of the prion protein from the C-terminal domain of recombinant murine prion protein mPrP-(121–231). *J Biol Chem* **281**: 26121–26128
- Ortega Z, Díaz-Hernández M, Maynard CJ, Hernández F, Dantuma NP, Lucas JJ (2010) Acute polyglutamine expression in inducible mouse model unravels ubiquitin/proteasome system impairment and permanent recovery attributable to aggregate formation. *J Neurosci* **30**: 3675–3688
- Osmulski PA, Hochstrasser M, Gaczynska M (2009) A tetrahedral transition state at the active sites of the 20S proteasome is coupled to opening of the alpha-ring channel. *Structure* **17**: 1137–1147
- Pagano M, Tam SW, Theodoras AM, Beer-Romero P, Del Sal G, Chau V, Yew PR, Draetta GF, Rolfe M (1995) Role of the ubiquitin-proteasome pathway in regulating abundance of the cyclin-dependent kinase inhibitor p27. *Science* **269**: 682–685
- Palombella VJ, Rando OJ, Goldberg AJ, Maniatis T (1994) The ubiquitin-proteasome pathway is required for processing the NF-kappa B1 precursor protein and the activation of NF-kappa B. *Cell* **78**: 773–785
- Perkins ND, Gilmore TD (2006) Good cop bad cop: the different faces of NF-kappaB. *Cell Death Differ* **13**: 759–772
- Peth A, Besche HC, Goldberg AL (2009) Ubiquitinated proteins activate the proteasome by binding to Usp14/Ubp6 which causes 20S gate opening. *Mol Cell* **36**: 794–804
- Pickart CM, Cohen RE (2004) Proteasomes and their kin: proteases in the machine age. *Nat Rev Mol Cell Biol* **5**: 177–187
- Prusiner SB (1982) Novel proteinaceous infectious particles cause scrapie. *Science* **216**: 136–144
- Prusiner SB (1998) Prions. *Proc Natl Acad Sci USA* **95**: 13363–13383
- Quaglio E, Restelli E, Garofoli A, Dossena S, De Luigi A, Tagliavacca L, Imperiale D, Migheli A, Salmons M, Sitia R, Forloni G, Chiesa R (2011) Expression of mutant or cytosolic PrP in transgenic mice and cells is not associated with endoplasmic reticulum stress or proteasome dysfunction. *PLoS One* **6**: e19339
- Rabl J, Smith DM, Yu Y, Chang SC, Goldberg AL, Cheng Y (2008) Mechanism of gate opening in the 20S proteasome by the proteasomal ATPases. *Mol Cell* **30**: 360–368
- Rubinsztein DC (2006) The roles of intracellular protein-degradation pathways in neurodegeneration. *Nature* **443**: 780–786
- Smith DM, Chang SC, Park S, Finley D, Cheng Y, Goldberg AL (2007) Docking of the proteasomal ATPases' carboxyl termini in the 20S proteasome's alpha ring opens the gate for substrate entry. *Mol Cell* **27**: 731–744
- Smith DM, Kafri G, Cheng Y, Ng D, Walz T, Goldberg AL (2005) ATP binding to PAN or the 26S ATPases causes association with the 20S proteasome gate opening and translocation of unfolded proteins. *Mol Cell* **20**: 687–698
- Sokolowski F, Modler AJ, Masuch R, Zirwer D, Baier M, Lutsch G, Moss DA, Gast K, Naumann D (2003) Formation of critical oligomers is a key event during conformational transition of recombinant syrian hamster prion protein. *J Biol Chem* **278**: 40481–40492
- Tatzelt J, Schatzl HM (2007) Molecular basis of cerebral neurodegeneration in prion diseases. *FEBS J* **274**: 606–611
- Toyoshima H, Hunter T (1994) p27, a novel inhibitor of G1 cyclin-Cdk protein kinase activity, is related to p21. *Cell* **78**: 67–74
- Tseng BP, Green KN, Chan JL, Blurton-Jones M, LaFerla FM (2008) Abeta inhibits the proteasome and enhances amyloid and tau accumulation. *Neurobiol Aging* **29**: 1607–1618
- Whitby FG, Masters EI, Kramer L, Knowlton JR, Yao Y, Wang CC, Hill CP (2000) Structural basis for the activation of 20S proteasomes by 11S regulators. *Nature* **408**: 115–120
- Yu Y, Smith DM, Kim HM, Rodriguez V, Goldberg AL, Cheng Y (2010) Interactions of PAN's C-termini with archaeal 20S proteasome and implications for the eukaryotic proteasome-ATPase interactions. *EMBO J* **29**: 692–702